Bio-Design and Manufacturing (2022) 5:607–616
https://doi.org/10.1007/s42242-022-00195-2

PERSPECTIVE

Recent progress on microfluidic devices with incorporated 1D nanostructures for enhanced extracellular vesicle (EV) separation

Yuting Xiong[1,2] · Hanyue Kang[1,2] · Hongzhao Zhou[3,4] · Liang Ma[3,4] · Xiaobin Xu[1,2]

Received: 12 October 2021 / Accepted: 27 February 2022 / Published online: 6 May 2022

Graphic abstract

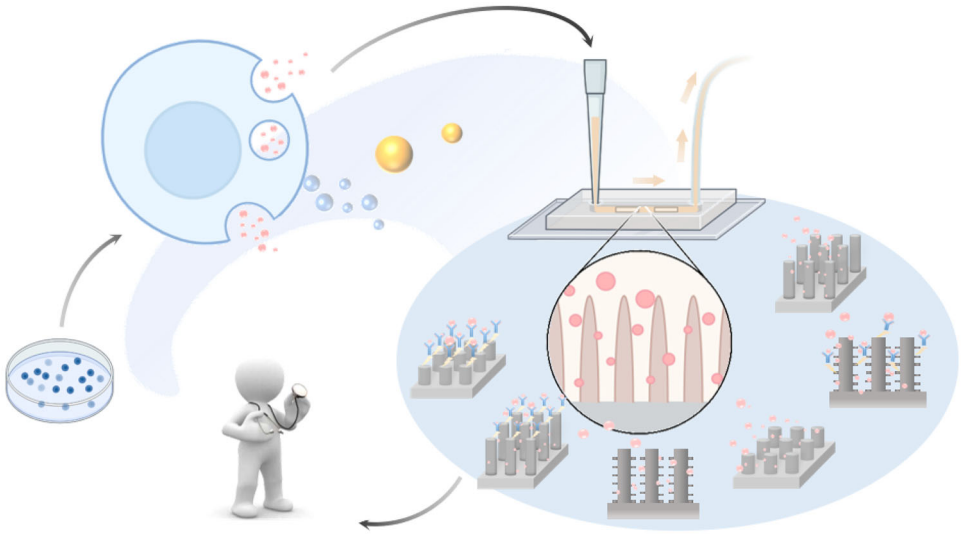

Introduction

Extracellular vesicles (EVs) are lipid-bound vesicles secreted by cells into the extracellular space. There are three types of EVs, including exosomes (30–150 nm) [1], microvesicles (100–1000 nm), and apoptotic bodies (50–4000 nm). EVs are also important intercellular communication carriers in many physiological and pathological processes such as immune response, tumor invasion, and metastasis [2, 3]. EVs circulate in various body fluids (e.g., peripheral blood and urine), while carrying genetic information (e.g., proteins and nucleic acids) from the parent cells [2, 4, 5]. Thus, their source can be identified through gene analysis [6–10].

As a result, the analysis of EVs is very useful for disease diagnosis, treatment, and prognostic evaluation, for example in cardiovascular diseases [11–13], cancer [14, 15], pathogen

Yuting Xiong and Hanyue Kang have contributed equally to this work.

✉ Liang Ma
liangma@zju.edu.cn

✉ Xiaobin Xu
xiaobinxu@tongji.edu.cn

1 Key Laboratory of Advanced Civil Engineering Materials of Ministry of Education, Shanghai Key Lab of D&A for Metal-Functional Materials, School of Materials Science and Engineering, Tongji University, Shanghai 201804, China

2 Institute for Advanced Study, Tongji University, Shanghai 201804, China

3 State Key Laboratory of Fluid Power and Mechatronic Systems, Zhejiang University, Hangzhou 310058, China

4 School of Mechanical Engineering, Zhejiang University, Hangzhou 310058, China

infection [16], pregnancy complications [17], and neurodegenerative diseases [18, 19]. Recently, EVs were discovered to have potential applications in personalized drug delivery [20–22].

However, due to the much smaller size of EVs (tens of nm) compared to regular red blood cells (6–8 microns), conventional centrifugation (about 10,000 g or less) cannot separate them from body fluid. Thus, simple, efficient, high-throughput, and specific separation of EVs remains a great challenge.

So far, tremendous efforts have been made to develop effective EV separation methods. Among them, ultracentrifugation (about 100,000 g or larger) is a straightforward and high-throughput physical separation approach [23]; however, it requires expensive ultracentrifugation equipment, multiple centrifugation steps, and large sample volumes, while affording relatively low separation efficiency [24, 25]. Other physical strategies, such as ultrafiltration and polymer-based precipitation approaches, are facile, are of low cost, and have flexible EV size options, but cause issues with the purity and integrity of EVs due to non-specific capture and membrane blocking [26, 27]. Immunocapture approaches are based on a specific chemical bonding mechanism, which allows for specific EV capture at high purity. However, they have issues like limited antibody availability, low yield, and high cost [28]. A summary of the above-described approaches is given in Table 1.

Recently, significant progress has been made on microfluidic-based EV isolation approaches, which offer improved separation efficiency, reduced processing time, and the ability to meet sample volume requirements [29, 30]. Previously, the laminar and uniaxial flow in conventional planar substrate-based microfluidic devices commonly resulted in limited interaction between the particles and the device surface [31, 32]. Today, non-planar microfluidic devices with incorporated nanostructure substrates have been developed and exhibit promising EV capture performance. The incorporated nanostructures not only break up unwanted streamlines in the microchannels, but also increase the specific surface area, and can be designed to match the dimensions of EVs to further increase the EV capture efficiency [33–36].

Among the different nanostructures, ordered arrays of one-dimensional (1D) nanostructures are frequently reported as effective for EV separation applications. The 1D nanostructure arrays have the following key features: dimensions that match EVs, the capacity to be modified with EV probes, and the capacity to be incorporated into microfluidic devices for high-throughput EV capture.

In this article, we focus on the recent progress of microfluidic devices with incorporated 1D nanostructures for enhanced EV separation. Note that, based on the morphologies of the 1D nanostructures, we roughly categorize them into three major types, as shown in Fig. 1: nanorods, nanowires, and three-dimensional (3D) nanostructures. In

Table 1 Summary of different extracellular vesicle (EV) isolation methods

Strategy	Approach/substrates	Separation mechanism	Benefits	Limitations
Conventional approaches	Ultracentrifugation [24, 25]	Size density	Straightforward High throughput	Long processing time Low purity and recovery Large sample consumption
	Ultra-filtration [26, 27]	Size	Facile, low cost, and rapid Flexible size options	EV deformation and lysis Membrane blocking
	Immunocapture [28]	Affinity	High specificity High purity	Limited antibody availability Low yield and high cost
Microfluidic with micro-/nanostructure (physical approach)	DLD [38, 39, 45] Nanowires [60, 70] Secondary structures [79]	Size surface charge	Label-free Rapid process Little damage to EVs	Clogging risk Nanofabrication required Low specificity and purity
Microfluidic with micro-/nanostructure (chemical approach)	Nanorods [47, 49, 56, 58] Nanowires [61, 63, 64] Secondary structure [77, 78, 80]	Size affinity	High specificity and purity Rapid process Little damage to EVs	Clogging risk Limited antibody availability Nanofabrication required

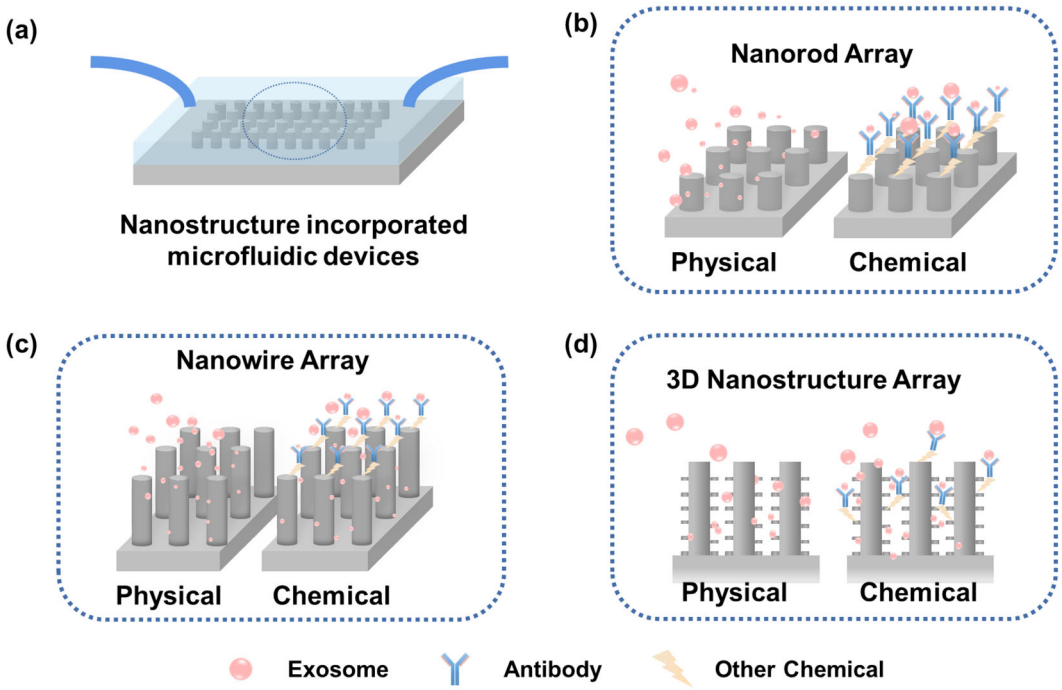

Fig. 1 Schematic illustrations of microfluidic chips with incorporated 1D nanostructure for EV capture (**a**), 1D nanorod arrays (**b**), 1D nanowire arrays (**c**), and 3D hierarchical nanostructure arrays (**d**)

addition, both physical and chemical (with EV probes) capturing mechanisms for these three types are described in detail with examples in the following sections.

Microfluidic devices with incorporated nanorod arrays

Nanorods are generally considered to be low-aspect-ratio 1D nanostructures (Fig. 1b). Nanorod arrays can be fabricated by nanolithography, such as photography, e-beam lithography, and nanosphere lithography [37–43]. When incorporated into a microfluidic device, these arrays can be used to generate chaotic flow within the microchannels to promote physical interactions between the EVs and nanorods for improved capture efficiency.

Nanorod arrays for physical separation of EVs

As shown in Fig. 2a, one typical physical separation mechanism of microfluidic devices with incorporated nanorod arrays is deterministic lateral displacement (DLD), which is a particle size-based physical mechanism [39]. In DLD, particles with diameters (D_p) larger than the critical cut-off diameter (D_c) continuously migrate toward the nanorods (bump mode), while smaller ones follow the fluid streamlines (zigzag mode). As a result, the trajectory and outlet of particle separation vary with different sizes.

For example, Huang et al. reported a DLD microfluidic device for particle isolation [44]. Each column of nanorods was positioned laterally by a designed distance, and at a designed angle facing the liquid flow direction. In the gaps between the nanorods, particles were successfully gradually separated according to their size.

In addition, nanorod arrays with designed gap sizes can physically separate EVs through size sorting. For instance, Wunsch et al. reported nano-DLD arrays for sorting and collection of EVs (from 20 to 140 nm) through controlled nanorod gap sizes (from 25 to 235 nm) at a small flow rate of about 0.2 μL/h, as shown in Fig. 2a [39]. Smith et al. further demonstrated a higher flow rate of 900 μL/h by integrating 1024 nano-DLD arrays into a single device, as shown in Fig. 2b [38]. The isolation mechanism supplied the sample to eight rows of DLD arrays along the inlet bus network. Larger particles ($D_p > D_c$) were enriched and exited from the bump outlet. Concurrently, smaller particles ($D_p < D_c$) exited from the zigzag outlets located on the back of the chip.

A challenge still exists with nano-DLD chips, namely that high pressures above 200 kPa are commonly required to transport EVs across the nanorod array. To address this limitation, Hattori et al. introduced electroosmotic flow (EOF) to nano-DLD chips [45] (Fig. 2c). This was realized by applying an electric field through the reservoirs to generate gradient electric fields, while EOF controlled the flow of negatively charged EVs for separation and enrichment.

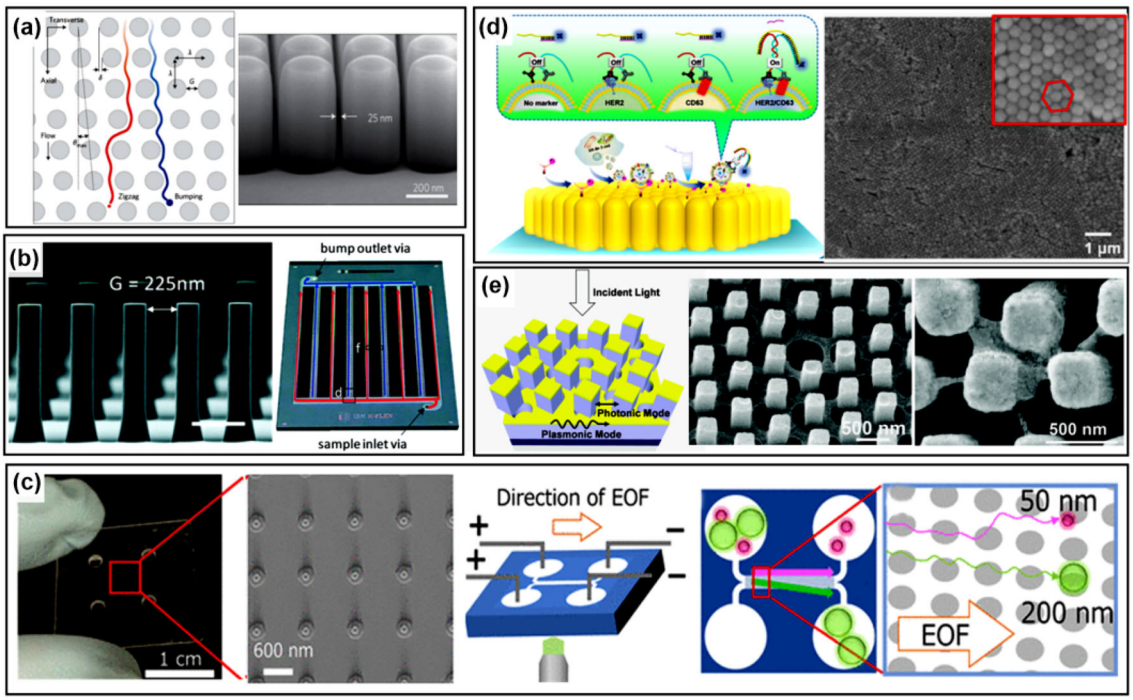

Fig. 2 Microfluidic devices with incorporated nanorod arrays. **a, b** Deterministic lateral displacement (DLD) for EV sorting (**a** is reproduced from Ref. [39], Copyright 2018, with permission from Royal Society of Chemistry; **b** is reproduced from Ref. [38], Copyright 2016, with permission from Springer Nature). **c** Electroosmotic-flow-based nano-DLD chip for nanoparticle control (reproduced from Ref. [45], Copyright 2019, with permission from American Chemical Society). **d** Au nanorod array for EV capture and detection (reproduced from Ref. [49], Copyright 2021, with permission from American Chemical Society). **e** 3D plasmonic photonic biosensor for EV capture and detection (reproduced from Ref. [56], Copyright 2018, with permission from RSC Pub)

Chemically modified nanorod arrays for enhanced separation of EVs

Although nanorod-based DLD chips were an advance in efficient EV separation, they cannot identify the types or source cells of EVs. Thus, additional chemical modifications are needed to capture target EVs of interest (Fig. 1b). The underlying principle of chemically modified capture is based on the binding interactions between the exosome surface membrane-bound proteins and the specific antibodies on the surface of the microfluidic devices. Studies have revealed that specific proteins (e.g., CD9, CD63, and EpCAM) of exosomes can serve as binding targets, when the corresponding specific capture probes (e.g., anti-CD9, anti-CD63, and anti-EpCAM antibodies) are modified on the nanorod surfaces [46].

For example, Lv et al. reported a simple and robust plasmonic biosensor array to detect exosomes down to 1 ng/mL with a small sample volume of 50 μL [47]. They applied anti-CD63 antibodies on ordered gold nanorod arrays to capture target exosomes containing CD63 protein antibodies. A smaller sample volume of 50 μL and a short detection time of about 4 hours was realized, compared with the standard ELISA (enzyme-linked immunosorbent assays) approach [48]. Likewise, Wang et al. improved another ultra-sensitive SERS (surface enhanced Raman spectrum) sensor to detect exosomes secreted by specific cells, as shown in Fig. 2d [49]. In their study, vertically aligned plasmonic Au nanorod arrays were combined with a DNA colocalization-dependent system to detect EVs optically. This technology enables the specific detection of exosomes secreted by SK-Br-3 cells in the cell culture medium (including SK-Br-3, RAW, HEK-293T, HeLa, and HepG2).

Nevertheless, plasmonic nanostructures such as Au nanorods [50, 51] and nanoholes [52] only couple with adjacent nanostructures in the two-dimensional region, which limits their sensitivity and figure of merit (FOM). Furthermore, the radiant dumping effect of the super-radiation plasma mode also reduces the FOM of the resonance peak spectrum [53]. Studies have shown that the complex plasma layer can enhance detection sensitivity [54, 55]. To improve the sensitivity, Zhu et al. used reverse nanoimprint lithography to fabricate 3D photonic crystal nanostructures with point defect cavities [56], which increased the sensing area and obtained a detection range from 10^4–10^{11} particles/mL (Fig. 2e), broader than in conventional nanoparticle tracking analysis (2×10^8 to 2×10^9 particles/mL) [57]. Other strategies, such as lipid nanoprobes and functionalized

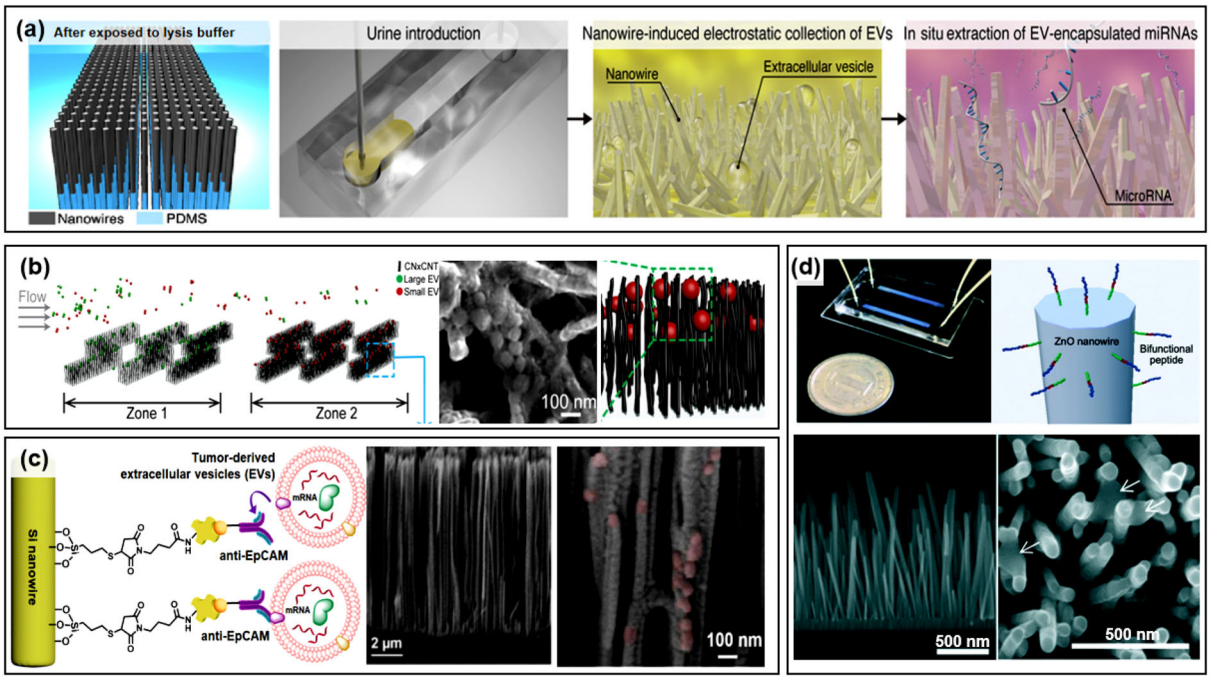

Fig. 3 Microfluidic devices with incorporated nanowires. **a** ZnO/Al_2O_3 core–shell devices collect urine EVs through an induced electrostatic effect followed by extraction of miRNAs (reproduced from Ref. [60] under Creative Commons license CC BY-NC 4.0). **b** Devices with herringbone-aligned carbon nanotube arrays for size-selective EV separation (reproduced from Ref. [70], Copyright 2020, with permission from American Chemical Society). **c** Devices with anti-EpCAM grafted Si nanowire arrays for immunoaffinity capture of EVs (reproduced from Ref. [63], Copyright 2019, with permission from American Chemical Society). **d** Devices with bifunctional peptide-modified ZnO nanowire arrays for cancer-derived EV capture (reproduced from Ref. [61], Copyright 2021, with permission from Royal Society of Chemistry)

silica nanorods, have also been reported for detection of EVs through DNA analysis via ddPCR [58].

Microfluidic devices with incorporated nanowires

Nanowires are high-aspect-ratio 1D nanostructures which generally have a larger specific surface area than nanorods, and thus more antibody binding sites. Similar to nanorod arrays, they can be incorporated into microfluidic devices for enhanced EV capture. Materials with good biocompatibility, such as ZnO [59–61], Si [62–64], and TiO_2 [65], are used to construct the nanowires. The gaps among the nanowires can be designed and controlled to match the EV size to facilitate physical separation [66].

Nanowire arrays for physical separation of EVs

Similar to nanorod arrays, the physical separation mechanism of nanowires mainly relies on the size effect and electrostatic adsorption (Fig. 1c) [67].

For instance, EVs in the urine are known to be difficult to separate due to being present only in trace amounts [68, 69]. Yasui et al. found that urine EVs and ZnO/Al_2O_3 nanowires had opposite surface charges at pH values of 6–8 [60]. Therefore, they integrated the nanowires into a microfluidic device and achieved a high EV capture efficiency (> 99%) through the electrostatic interaction between the nanowires and EVs. These nanowires also showed decent mechanical stability in the lysis buffer and during the extraction of miRNAs with different sequences (about 1000 species) (Fig. 3a).

As shown in Fig. 3b, Yeh et al. reported herringbone-aligned N-doped multiwalled carbon nanotube arrays (inter-tube distance: from 22 to 720 nm) for physical separation of EVs [70]. The fluid microvortex caused by the herringbone carbon nanotube array was able to enhance the mixing of circulating medium, allowing EV separation with size selectivity [30, 71].

Although nanowire arrays can capture EVs with unknown antibodies and maintain their integrity, unwanted clogging is frequently reported, which would lead to a saturation limit and thus reduce EV purity.

Chemically modified nanowire arrays for enhanced separation of EVs

Chemically modified nanowire arrays have also been reported for EV capture, with the added feature of EV specificity (Fig. 1c). For example, Dong et al. reported an anti-EpCAM antibody-grafted Si nanowire chip for efficient capture of tumor-derived EVs [63] (Fig. 3c). The large specific surface area of the nanowires and the spiral flow introduced by the herringbone micropatterns significantly improved EV capture efficiency. Under optimal conditions, the RNA recovery rate reached $(82 \pm 8)\%$. On the same chip, they further combined covalent chemical mediation (a type of click chemistry) with specific antibodies to capture and release specific EVs (hepatocellular carcinoma) [63, 64]. It is noteworthy that compared to immunoaffinity, click chemistry results in superior EV recovery purity, as the release of EVs can be simply achieved through disulfide cleavage.

Captured EVs often need to be released for subsequent bioanalysis and application. However, unmodified or antibody-modified nanowires must often be dissolved in acidic solutions for EV release. As one possible solution, Suwatthanarak et al. reported bifunctional peptide-modified ZnO nanowire arrays for capture and release of EVs (Fig. 3d) [61]. The captured exosomes can be released by adding neutral salt, without damaging the nanowires.

Microfluidic devices with incorporated 3D nanostructure arrays for enhanced separation of EVs

As illustrated in Fig. 1d, the type of 3D nanostructure we consider here is a combination of base microstructures (either 1D microrods or network-like structures) and secondary nanostructures (nanorods or nanowires). These 3D nanostructures have increased specific surface area to provide more EV binding sites than those without secondary structures. As a result of enhanced interactions between the microfluidic device and EVs, the EV capture efficiency has been improved as well [72–76].

For instance, Chen et al. reported a 3D scaffold chip for EV capture [77] (Fig. 4a). ZnO nanowires were vertically grown on a network-like porous polymeric scaffold. The chaotic and vortex mixing effect induced by interconnected micropores increased the interaction between EVs and nanowires. Meanwhile, the densely arranged nanowires not only grafted with antibodies for specific binding, but also improved capture efficiency through physical size sorting. Ultimately, the isolated exosomes could be released simply by pH adjustment. In another case, Wang et al. reported polymer micropillar arrays coated with secondary carbon nanotubes for capture and release of EVs (Fig. 4b) [78]. After conjugating the carbon nanotubes with an antibody, they achieved a good EV recovery rate of about 90%.

As described in "Microfluidic devices with incorporated nanorod arrays", nanorod arrays have been incorporated into microfluidic chips for EV capture and isolation. To further improve capture efficiency, secondary smaller nanostructures can be added to nanorod arrays to generate even higher specific surface area. As shown in Fig. 4c, Wang et al. fabricated ciliated silicon nanorod arrays through silicon micromachining and Ag nanoparticle-assisted chemical etching [79]. Ciliated nanorod at a distance of 30–120 nm can provide abundant EV binding sites. In addition, the cilia can be dissolved in PBS (phosphate buffer saline) buffer to release and recover high-purity liposomes, maintaining their integrity. When injecting a 30-μL sample, the retention rate of 83 nm liposomes reached 60%.

To avoid EV saturation of the physical size separation-based platform, Qi et al. developed a high-capacity microfluidic device with a microcolumn area of 627 mm [2, 80] (Fig. 4d). The biotinylated anti-CD63 antibody was stably immobilized on the microcolumn, and the retention rate of exosomes reached 75% due to antibody-specific capture. It is worth noting that the improved device can also be used to analyze exosomes derived from multidrug-resistant (MDR) cancer cells treated with drug-loaded nanoparticles, which is promising for the development of nanotherapy to overcome MDR.

Summary and perspective

In summary, multiple studies have shown that microfluidic devices with incorporated 1D nanostructures increase molecular binding surface area. They produce a combined fluid mixing effect that results in enhanced EV capture, separation, and detection. Table 2 summarizes and compares the aforementioned microfluidic EV isolation methods in detail. With continuous advances in materials, structures, and microfluidic design, there is no doubt about the great potential of microfluidics for clinical applications. We expect the commercialization of microfluidics that incorporate nanostructures to promote the development of clinical testing methods toward miniaturization, rapidity, high throughput, portability, and automation. We believe the widespread use of "labs-on-a-chip" is just around the corner.

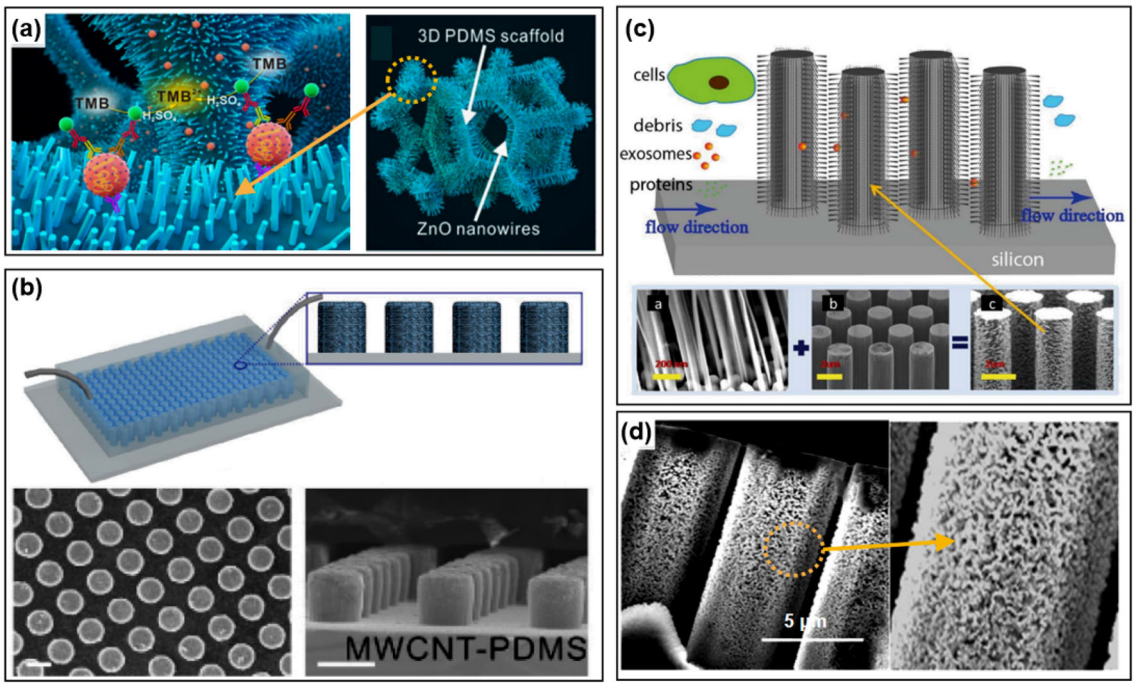

Fig. 4 Microfluidic devices with incorporated 3D nanostructures. **a** 3D scaffold with secondary nanostructure (ZnO nanowire) (reproduced from Ref. [77], Copyright 2018, with permission from Elsevier). **b** Multiwalled carbon nanotubes and modified polymer micropillars (reproduced from Ref. [78], Copyright 2017, with permission from American Chemical Society). Scale bar, 50 μm. **c, d** Ciliated microrod arrays (reproduced from Ref. [79], Copyright 2013, with permission from Royal Society of Chemistry; reproduced from Ref. [80], Copyright 2019, with permission from Springer Nature)

Table 2 Typical microfluidic devices with incorporated 1D nanostructure arrays for extracellular vesicle (EV) capture and analysis

Structure	Modification	EV source	Volume	Throughput	Capture efficiency	Ref.
Nanorod	None	Urine (human)	10 μL	0.2 nL/min	n/a	[39]
	None	Serum (human)	480 μL	8 μL/min	~50%	[38]
	None	MDA-MB-231	n/a	0.3 nL/min	n/a	[45]
	Anti-CD63	COLO1	50 μL	n/a	n/a	[47]
	EpCAM aptamer	SK-Br-3	20 μL	n/a	n/a	[49]
	Anti-EpCAM	Fibroblast L	10 μL	n/a	n/a	[56]
	Lipid nanoprobe	MDA-MB-231 PANC-1	<2000 μL	40 μL/min	~29%	[58]
Nanowire	None	Primary glial cells (mouse)	n/a	500 μL/min	~50%	[70]
	None	Urine	1000 μL	50 μL/min	~99%	[60]
	Anti-EpCAM	NSCLC	100 μL	0.2 mL/h	~82%	[63]
	Anti-EpCAM/ ASGPR1/CD147	HepG2	100 μL	1 mL/h	~83%	[64]
	Peptide	MDA-MB-231	1000 μL	50 μL/min	n/a	[61]
3D hybrid nanostructure	Anti-CD63	MCF-7	n/a	30 μL/ min	n/a	[77]
		MDA-MB-231	n/a	10 μL/min	~75%	[80]
		HUVECs	400 μL	1 mL/h	~90%	[78]

n/a: Did not provide

Acknowledgements This work was financially supported by the Shanghai Municipal Science and Technology Major Project (No. 2021SHZDZX0100) and the Fundamental Research Funds for the Central Universities, China. Hongzhao Zhou and Liang Ma are grateful for a grant from the National Natural Science Foundation of China (No. 51875518).

Author contributions All authors have read and agreed to the published version of the manuscript. YTX and HYK were involved in writing (original draft, and review and editing); HZZ and LM were involved in supervision; and XBX was involved in supervision and writing (review and editing and visualization).

Declarations

Conflict of interest The authors declare that they have no conflict of interest.

Ethical approval This study does not contain any studies with human or animal subjects performed by any of the authors.

References

1. Simpson RJ, Jensen SS, Lim JW (2008) Proteomic profiling of exosomes: current perspectives. Proteomics 8(19):4083–4099. https://doi.org/10.1002/pmic.200800109
2. Colombo M, Raposo G, Théry C (2014) Biogenesis, secretion, and intercellular interactions of exosomes and other extracellular vesicles. Annu Rev Cell Dev Biol 30:255–289. https://doi.org/10.1146/annurev-cellbio-101512-122326
3. Théry C, Ostrowski M, Segura E (2009) Membrane vesicles as conveyors of immune responses. Nat Rev Immunol 9(8):581–593. https://doi.org/10.1038/nri2567
4. Lin B, Lei Y, Wang J et al (2021) Microfluidic-based exosome analysis for liquid biopsy. Small Methods 5(3):e2001131. https://doi.org/10.1002/smtd.202001131
5. Subra C, Perret LK, B, et al (2007) Exosome lipidomics unravels lipid sorting at the level of multivesicular bodies. Biochimie 89:205–212. https://doi.org/10.1016/j.biochi.2006.10.014
6. El Andaloussi S, Mäger I, Breakefield XO et al (2013) Extracellular vesicles: biology and emerging therapeutic opportunities. Nat Rev Drug Discov 12(5):347–357. https://doi.org/10.1038/nrd3978
7. Ronquist GK, Larsson A, Stavreus-Evers A et al (2012) Prostasomes are heterogeneous regarding size and appearance but affiliated to one DNA-containing exosome family. Prostate 72(16):1736–1745. https://doi.org/10.1002/pros.22526
8. Valadi H, Ekström K, Bossios A et al (2007) Exosome-mediated transfer of mRNAs and microRNAs is a novel mechanism of genetic exchange between cells. Nat Cell Biol 9(6):654–659. https://doi.org/10.1038/ncb1596
9. Bullock MD, Silva AM, Kanlikilicer-Unaldi P et al (2015) Exosomal non-coding RNAs: diagnostic, prognostic and therapeutic applications in cancer. Noncoding RNA 1(1):53–68. https://doi.org/10.3390/ncrna1010053
10. Lin S, Yu Z, Chen D et al (2020) Progress in microfluidics-based exosome separation and detection technologies for diagnostic applications. Small 16(9):e1903916. https://doi.org/10.1002/smll.201903916
11. Castaño C, Kalko S, Novials A et al (2018) Obesity-associated exosomal miRNAs modulate glucose and lipid metabolism in mice. Proc Natl Acad Sci USA 115(48):12158–12163. https://doi.org/10.1073/pnas.1808855115
12. Jansen F, Li Q (2017) Exosomes as diagnostic biomarkers in cardiovascular diseases. Adv Exp Med Biol 998:61–70. https://doi.org/10.1007/978-981-10-4397-0_4
13. Zhang Y, Hu YW, Zheng L et al (2017) Characteristics and roles of exosomes in cardiovascular disease. DNA Cell Biol 36(3):202–211. https://doi.org/10.1089/dna.2016.3496
14. Chen G, Huang AC, Zhang W et al (2018) Exosomal PD-L1 contributes to immunosuppression and is associated with anti-PD-1 response. Nature 560(7718):382–386. https://doi.org/10.1038/s41586-018-0392-8
15. Jara-Acevedo R, Campos-Silva C, Valés-Gómez M et al (2019) Exosome beads array for multiplexed phenotyping in cancer. J Proteomics 198:87–97. https://doi.org/10.1016/j.jprot.2018.12.023
16. Pegtel DM, Cosmopoulos K, Thorley-Lawson DA et al (2010) Functional delivery of viral miRNAs via exosomes. Proc Natl Acad Sci USA 107(14):6328–6333. https://doi.org/10.1073/pnas.0914843107
17. Salomon C, Guanzon D, Scholz-Romero K et al (2017) Placental exosomes as early biomarker of preeclampsia: potential role of exosomal microRNAs across gestation. J Clin Endocrinol Metab 102(9):3182–3194. https://doi.org/10.1210/jc.2017-00672
18. Kanninen KM, Bister N, Koistinaho J et al (2016) Exosomes as new diagnostic tools in CNS diseases. Biochim Biophys Acta 1862(3):403–410. https://doi.org/10.1016/j.bbadis.2015.09.020
19. Tassew NG, Charish J, Shabanzadeh AP et al (2017) Exosomes mediate mobilization of autocrine Wnt10b to promote axonal regeneration in the injured CNS. Cell Rep 20(1):99–111. https://doi.org/10.1016/j.celrep.2017.06.009
20. Alvarez-Erviti L, Seow Y, Yin H et al (2011) Delivery of siRNA to the mouse brain by systemic injection of targeted exosomes. Nat Biotechnol 29(4):341–345. https://doi.org/10.1038/nbt.1807
21. Haney MJ, Klyachko NL, Zhao Y et al (2015) Exosomes as drug delivery vehicles for Parkinson's disease therapy. J Contr Release 207:18–30. https://doi.org/10.1016/j.jconrel.2015.03.033
22. van den Boorn JG, Schlee M, Coch C et al (2011) SiRNA delivery with exosome nanoparticles. Nat Biotechnol 29(4):325–326. https://doi.org/10.1038/nbt.1830
23. Livshits MA, Khomyakova E, Evtushenko EG et al (2015) Isolation of exosomes by differential centrifugation: theoretical analysis of a commonly used protocol. Sci Rep 5:17319. https://doi.org/10.1038/srep17319
24. Lamparski HG, Metha-Damani A, Yao JY et al (2002) Production and characterization of clinical grade exosomes derived from dendritic cells. J Immunol Methods 270(2):211–226. https://doi.org/10.1016/s0022-1759(02)00330-7
25. Théry C, Amigorena S, Raposo G et al (2006) Isolation and characterization of exosomes from cell culture supernatants and biological fluids. Curr Protoc Cell Biol Chapter 3:Unit 3.22. https://doi.org/10.1002/0471143030.cb0322s30
26. Guo SC, Tao SC, Dawn H (2018) Microfluidics-based on-a-chip systems for isolating and analysing extracellular vesicles. J Extracell Vesicles 7(1):1508271. https://doi.org/10.1080/20013078.2018.1508271
27. Vlassov AV, Magdaleno S, Setterquist R et al (2012) Exosomes: current knowledge of their composition, biological functions, and diagnostic and therapeutic potentials. Biochim Biophys Acta 1820(7):940–948. https://doi.org/10.1016/j.bbagen.2012.03.017
28. Witwer KW, Buzás EI, Bemis LT et al (2013) Standardization of sample collection, isolation and analysis methods in extracellular vesicle research. J Extracell Vesicles 2:20360. https://doi.org/10.3402/jev.v2i0.20360
29. Stott SL, Hsu CH, Tsukrov DI et al (2010) Isolation of circulating tumor cells using a microvortex-generating herringbone-chip. Proc Natl Acad Sci USA 107(43):18392–18397. https://doi.org/10.1073/pnas.1012539107

30. Liga A, Vliegenthart ADB, Oosthuyzen W, Dear JW, Kersaudy-Kerhoas M (2015) Exosome isolation: a microfluidic road-map. Lab Chip 15:2388–2394
31. Kabedev A, Ross-Lonergan M, Lobaskin V (2017) Hydrodynamic lift forces on solutes in a tilted nanopillar array: a computer simulation study. Electrophoresis 38(19):2479–2487. https://doi.org/10.1002/elps.201700130
32. Tang Q, Yang X, Xuan C et al (2020) Generation of microfluidic gradients and their effects on cells behaviours. Bio-Des Manuf 3:427–431. https://doi.org/10.1007/s42242-020-00093-5
33. Xiang C, Kung SC, Taggart DK et al (2008) Lithographically patterned nanowire electrodeposition: a method for patterning electrically continuous metal nanowires on dielectrics. ACS Nano 2(9):1939–1949. https://doi.org/10.1021/nn800394k
34. Huang Z, Zhang X, Reiche M et al (2008) Extended arrays of vertically aligned sub-10 nm diameter [100] Si nanowires by metal-assisted chemical etching. Nano Lett 8(9):3046–3051. https://doi.org/10.1021/nl802324y
35. Albuschies J, Vogel V (2013) The role of filopodia in the recognition of nanotopographies. Sci Rep 3:1658. https://doi.org/10.1038/srep01658
36. Yoon HJ, Kozminsky M, Nagrath S (2014) Emerging role of nanomaterials in circulating tumor cell isolation and analysis. ACS Nano 8(3):1995–2017. https://doi.org/10.1021/nn5004277
37. Zeming KK, Ranjan S, Zhang Y (2013) Rotational separation of non-spherical bioparticles using I-shaped pillar arrays in a microfluidic device. Nat Commun 4:1625. https://doi.org/10.1038/ncomms2653
38. Smith JT, Wunsch BH, Dogra N et al (2018) Integrated nanoscale deterministic lateral displacement arrays for separation of extracellular vesicles from clinically-relevant volumes of biological samples. Lab Chip 18(24):3913–3925. https://doi.org/10.1039/c8lc01017j
39. Wunsch BH, Smith JT, Gifford SM et al (2016) Nanoscale lateral displacement arrays for the separation of exosomes and colloids down to 20 nm. Nat Nanotechnol 11(11):936–940. https://doi.org/10.1038/nnano.2016.134
40. Xu X, Yang Q, Wattanatorn N et al (2017) Multiple-patterning nanosphere lithography for fabricating periodic three-dimensional hierarchical nanostructures. ACS Nano 11(10):10384–10391. https://doi.org/10.1021/acsnano.7b05472
41. Shang Y, Chen Z, Zhang Z et al (2020) Heart-on-chips screening based on photonic crystals. Bio-Des Manuf 3:266–280. https://doi.org/10.1007/s42242-020-00073-9
42. Xu X, Liu W, Ji Z et al (2021) Large-area periodic organic–inorganic hybrid perovskite nanopyramid arrays for high-performance photodetector and image sensor applications. ACS Mater Lett 3:1189–1196. https://doi.org/10.1021/acsmaterialslett.1c00298
43. Liu W, Wang J, Xu X et al (2021) Single-step dual-layer photolithography for tunable and scalable nanopatterning. ACS Nano 15(7):12180–12188. https://doi.org/10.1021/acsnano.1c03703
44. Huang LR, Cox EC, Austin RH et al (2004) Continuous particle separation through deterministic lateral displacement. Science 304(5673):987–990. https://doi.org/10.1126/science.1094567
45. Hattori Y, Shimada T, Yasui T et al (2019) Micro- and nanopillar chips for continuous separation of extracellular vesicles. Anal Chem 91(10):6514–6521. https://doi.org/10.1021/acs.analchem.8b05538
46. Deng F, Miller J (2019) A review on protein markers of exosome from different bio-resources and the antibodies used for characterization. J Histotechnol 42(4):226–239. https://doi.org/10.1080/01478885.2019.1646984
47. Lv X, Geng Z, Su Y et al (2019) Label-free exosome detection based on a low-cost plasmonic biosensor array integrated with microfluidics. Langmuir 35(30):9816–9824. https://doi.org/10.1021/acs.langmuir.9b01237
48. Duan L, Wang Y, Li SS et al (2005) Rapid and simultaneous detection of human hepatitis B virus and hepatitis C virus antibodies based on a protein chip assay using nano-gold immunological amplification and silver staining method. BMC Infect Dis 5:53. https://doi.org/10.1186/1471-2334-5-53
49. Wang J, Xie H, Ding C (2021) Designed Co-DNA-locker and ratiometric SERS sensing for accurate detection of exosomes based on gold nanorod arrays. ACS Appl Mater Interf 13(28):32837–32844. https://doi.org/10.1021/acsami.1c09388
50. Liu F, Wong MM, Chiu SK et al (2014) Effects of nanoparticle size and cell type on high sensitivity cell detection using a localized surface plasmon resonance biosensor. Biosens Bioelectron 55:141–148. https://doi.org/10.1016/j.bios.2013.11.075
51. Zhao X, Wong MM, Chiu SK et al (2015) Effects of three-layered nanodisk size on cell detection sensitivity of plasmon resonance biosensors. Biosens Bioelectron 74:799–807. https://doi.org/10.1016/j.bios.2015.07.022
52. Bochenkov VE, Frederiksen M, Sutherland DS (2013) Enhanced refractive index sensitivity of elevated short-range ordered nanohole arrays in optically thin plasmonic Au films. Opt Express 21(12):14763–14770. https://doi.org/10.1364/OE.21.014763
53. Sonnefraud Y, Verellen N, Sobhani H et al (2010) Experimental realization of subradiant, superradiant, and fano resonances in ring/disk plasmonic nanocavities. ACS Nano 4(3):1664–1670. https://doi.org/10.1021/nn901580r
54. Ai B, Wang L, Möhwald H et al (2015) Confined surface plasmon sensors based on strongly coupled disk-in-volcano arrays. Nanoscale 7(6):2317–2324. https://doi.org/10.1039/c4nr05206d
55. Zhu S, Li H, Yang M et al (2016) High sensitivity plasmonic biosensor based on nanoimprinted quasi 3D nanosquares for cell detection. Nanotechnology 27(29):295101. https://doi.org/10.1088/0957-4484/27/29/295101
56. Zhu S, Li H, Yang M et al (2018) Highly sensitive detection of exosomes by 3D plasmonic photonic crystal biosensor. Nanoscale 10(42):19927–19936. https://doi.org/10.1039/c8nr07051b
57. Vestad B, Llorente A, Neurauter A et al (2017) Size and concentration analyses of extracellular vesicles by nanoparticle tracking analysis: a variation study. J Extracell Vesicles 6(1):1344087. https://doi.org/10.1080/20013078.2017.1344087
58. Wan Y, Maurer M, He HZ et al (2019) Enrichment of extracellular vesicles with lipid nanoprobe functionalized nanostructured silica. Lab Chip 19(14):2346–2355. https://doi.org/10.1039/c8lc01359d
59. Guo L, Shi Y, Liu X et al (2018) Enhanced fluorescence detection of proteins using ZnO nanowires integrated inside microfluidic chips. Biosens Bioelectron 99:368–374. https://doi.org/10.1016/j.bios.2017.08.003
60. Yasui T, Yanagida T, Ito S et al (2017) Unveiling massive numbers of cancer-related urinary-microRNA candidates via nanowires. Sci Adv 3(12):e1701133. https://doi.org/10.1126/sciadv.1701133
61. Suwatthanarak T, Thiodorus IA, Tanaka M et al (2021) Microfluidic-based capture and release of cancer-derived exosomes via peptide-nanowire hybrid interface. Lab Chip 21(3):597–607. https://doi.org/10.1039/d0lc00899k
62. Wang S, Wang H, Jiao J et al (2009) Three-dimensional nanostructured substrates toward efficient capture of circulating tumor cells. Angew Chem Int Ed Engl 48(47):8970–8973. https://doi.org/10.1002/anie.200901668
63. Dong J, Zhang RY, Sun N et al (2019) Bio-inspired NanoVilli chips for enhanced capture of tumor-derived extracellular vesicles: toward non-invasive detection of gene alterations in non-small cell lung cancer. ACS Appl Mater Interf 11(15):13973–13983. https://doi.org/10.1021/acsami.9b01406
64. Sun N, Lee YT, Zhang RY et al (2020) Purification of HCC-specific extracellular vesicles on nanosubstrates for early HCC detection by digital scoring. Nat Commun 11(1):4489. https://doi.org/10.1038/s41467-020-18311-0

65. Zhang N, Deng Y, Tai Q et al (2012) Electrospun TiO_2 nanofiber-based cell capture assay for detecting circulating tumor cells from colorectal and gastric cancer patients. Adv Mater 24(20):2756–2760. https://doi.org/10.1002/adma.201200155
66. Wendisch FJ, Abazari M, Mahdavi H et al (2020) Morphology-graded silicon nanowire arrays via chemical etching: engineering optical properties at the nanoscale and macroscale. ACS Appl Mater Interf 12(11):13140–13147. https://doi.org/10.1021/acsami.9b21466
67. Merchant ML, Rood IM, Deegens JKJ et al (2017) Isolation and characterization of urinary extracellular vesicles: implications for biomarker discovery. Nat Rev Nephrol 13(12):731–749. https://doi.org/10.1038/nrneph.2017.148
68. Hogan MC, Johnson KL, Zenka RM et al (2014) Subfractionation, characterization, and in-depth proteomic analysis of glomerular membrane vesicles in human urine. Kidney Int 85(5):1225–1237. https://doi.org/10.1038/ki.2013.422
69. Leiblich A (2017) Recent developments in the search for urinary biomarkers in bladder cancer. Curr Urol Rep 18(12):100. https://doi.org/10.1007/s11934-017-0748-x
70. Yeh YT, Zhou Y, Zou D et al (2020) Rapid size-based isolation of extracellular vesicles by three-dimensional carbon nanotube arrays. ACS Appl Mater Interf 12(11):13134–13139. https://doi.org/10.1021/acsami.9b20990
71. Stroock AD, Dertinger SK, Ajdari A et al (2002) Chaotic mixer for microchannels. Science 295(5555):647–651. https://doi.org/10.1126/science.1066238
72. Li Y, Xuan J, Song Y et al (2016) Nanoporous glass integrated in volumetric bar-chart chip for point-of-care diagnostics of non-small cell lung cancer. ACS Nano 10(1):1640–1647. https://doi.org/10.1021/acsnano.5b07357
73. Liu H, Ruan M, Xiao J et al (2018) TiO_2 nanorod arrays with mesoscopic micro-nano interfaces for in situ regulation of cell morphology and nucleus deformation. ACS Appl Mater Interf 10(1):66–74. https://doi.org/10.1021/acsami.7b11257
74. Song Y, Dong X, Shang D et al (2021) Unusual nanofractal microparticles for rapid protein capture and release. Small 17(36):e2102802. https://doi.org/10.1002/smll.202102802
75. Wang L, Liu H, Zhang F et al (2016) Smart thin hydrogel coatings harnessing hydrophobicity and topography to capture and release cancer cells. Small 12(34):4697–4701. https://doi.org/10.1002/smll.201601275
76. Yu X, Xia Y, Tang Y et al (2017) A nanostructured microfluidic immunoassay platform for highly sensitive infectious pathogen detection. Small 13(24):1700425. https://doi.org/10.1002/smll.201700425
77. Chen Z, Cheng SB, Cao P et al (2018) Detection of exosomes by ZnO nanowires coated three-dimensional scaffold chip device. Biosens Bioelectron 122:211–216. https://doi.org/10.1016/j.bios.2018.09.033
78. Wang J, Li W, Zhang L et al (2017) Chemically edited exosomes with dual ligand purified by microfluidic device for active targeted drug delivery to tumor cells. ACS Appl Mater Interf 9(33):27441–27452. https://doi.org/10.1021/acsami.7b06464
79. Wang Z, Wu HJ, Fine D et al (2013) Ciliated micropillars for the microfluidic-based isolation of nanoscale lipid vesicles. Lab Chip 13(15):2879–2882. https://doi.org/10.1039/c3lc41343h
80. Qi R, Zhu G, Wang Y et al (2019) Microfluidic device for the analysis of MDR cancerous cell-derived exosomes' response to nanotherapy. Biomed Microdev 21(2):35. https://doi.org/10.1007/s10544-019-0381-1